Kinetic properties and heme pocket structure of two domains of the polymeric hemoglobin of Artemia in comparison with the native molecule

Reference:

Akbari Borhani Heshmat, Berghmans Herald, Trashin Stanislav, De Wael Karolien, Fago Angela, Moens Luc, Habibi-Rezaei Mehran, Dewilde Sylvia.- Kinetic properties and heme pocket structure of two domains of the polymeric hemoglobin of Artemia in comparison with the native molecule

Biochimica et biophysica acta : proteins and proteomics - ISSN 1570-9639 - (2015), p. 1-10

DOI: http://dx.doi.org/doi:10.1016/j.bbapap.2015.05.007

Biochimica et Biophysica Acta xxx (2015) xxx–xxx

Contents lists available at ScienceDirect

Biochimica et Biophysica Acta

journal homepage: www.elsevier.com/locate/bbapap

Kinetic properties and heme pocket structure of two domains of the polymeric hemoglobin of *Artemia* in comparison with the native molecule

Heshmat Akbari Borhani [a,b], Herald Berghmans [b], Stanislav Trashin [c], Karolien De Wael [c], Angela Fago [d], Luc Moens [b], Mehran Habibi-Rezaei [a,e,*], Sylvia Dewilde [b,**]

[a] School of Biology, College of Science, University of Tehran, Tehran, Iran
[b] Department of Biomedical Sciences, University of Antwerp, Antwerp, Belgium
[c] Department of Chemistry, University of Antwerp, Antwerp, Belgium
[d] Department of Bioscience, Zoophysiology, Aarhus University, Aarhus, Denmark
[e] Nano-Biomedicine Center of Excellence, Nanoscience and Nanotechnology Research Center, University of Tehran, Tehran, Iran

ARTICLE INFO

Article history:
Received 6 February 2015
Received in revised form 30 April 2015
Accepted 14 May 2015
Available online xxxx

Keywords:
Artemia hemoglobin
Ligand binding kinetics
Heme pocket structure
Redox potential

ABSTRACT

In this project, we studied some physicochemical properties of two different globin domains of the polymeric hemoglobin of the brine shrimp *Artemia salina* and compared them with those of the native molecule. Two domains (*As*HbC1D1 and *As*HbC1D5) were cloned and expressed in BL21(DE3)pLysS strain of *Escherichia coli*. The recombinant proteins as well as the native hemoglobin (*Af*Hb) were purified from bacteria and frozen *Artemia*, respectively by standard chromatographic methods and assessed by SDS-PAGE. The heme environment of these proteins was studied by optical spectroscopy and ligand-binding kinetics (e.g. CO association and O_2 binding affinity) were measured for the two recombinant proteins and the native hemoglobin. This indicates that the CO association rate for *As*HbC1D1 is higher than that of *As*HbC1D5 and *Af*Hb, while the calculated P_{50} value for *As*HbC1D1 is lower than that of *As*HbC1D5 and *Af*Hb. The geminate and bimolecular rebinding parameters indicate a significant difference between both domains. Moreover, EPR results showed that the heme pocket in *Af*Hb is in a more closed conformation than the heme pocket in myoglobin. Finally, the reduction potential of −0.13 V versus the standard hydrogen electrode was determined for *Af*Hb by direct electrochemical measurements. It is about 0.06 V higher than the potential of the single domain *As*HbC1D5. This work shows that each domain in the hemoglobin of *Artemia* has different characteristics of ligand binding.

1. Introduction

Hemoglobins (Hbs) are a specific class of proteins consisting of a single or multiple globin chains. These globin chains display the specific globin fold consisting of 7 or 8 α-helical segments (indicated A to H) wrapped around a heme b moiety according to a 3-over-3 α-helical sandwich pattern [1,2]. The heme iron atom is penta- (F8His) or hexa-coordinate depending on the presence of an internal 6th ligand (usually E7His) [3,4]. Comparative studies demonstrate that Hbs occur in all kingdoms of life and that the canonical globin fold displays an extreme flexibility [4–7]. Due to the reactivity of the heme iron atom, globins are involved in a diversity of reactions varying e.g. from O_2 metabolism (O_2 sensing, carrying, storing) to redox chemistry (nitroso and oxidative stress metabolism) [8]. In some invertebrate classes (*Annelida*, *Mollusca*, *Crustacea*), Hbs occur as high M_r proteins dissolved in the extracellular fluid or hemolymph. Such high M_r is necessary e.g. to avoid pigment loss due to excretory filtration events. This high M_r is obtained either by disulfide bond based aggregation (e.g. in *Annelida*) or by the covalently concatenation of globin domains into polymeric globin chains (e.g. in *Mollusca*, *Crustacea*) [7].

An example of Hbs containing polymeric globin chains are those from the brine shrimp *Artemia*, a small branchiopod crustacean inhabiting worldwide diverse ponds with variations in O_2 partial pressure due to difference in salinity (e.g. up to 50% salinity) [9]. *Artemia* expresses genotypically four different globin chains (M_r ~160,000) namely C1, C2, T1 and T2 [10–12]. Structural analyses demonstrate that the T and C chains are ring-shaped polymers of nine genuine globin domains covalently joined by short inter-domain linkers (Fig. 1) [13]. All domains show different primary structures (identities: 23–39%)

* Correspondence to: M. Habibi-Rezaei, School of Biology, College of Science, University of Tehran, Tehran, Iran. Tel.: +98 21 61 11 32 14; fax: +98 21 66 49 29 92.
** Correspondence to: S. Dewilde, University of Antwerp, Universiteitsplein 1, 2610 Wilrijk, Belgium. Tel.: +32 3 265 23 23; fax: +32 3 265 22 48.
E-mail addresses: heshmat.akbariborhani@uantwerpen.be (H.A. Borhani), herald.berghmans@uantwerpen.be (H. Berghmans), stanislav.trashin@uanwerpen.be (S. Trashin), karolien.dewael@uantwerpen.be (K. De Wael), angela.fago@biology.au.dk (A. Fago), luc.moens@uantwerpen.be (L. Moens), mhabibi@ut.ac.ir (M. Habibi-Rezaei), sylvia.dewilde@uantwerpen.be (S. Dewilde).

http://dx.doi.org/10.1016/j.bbapap.2015.05.007
1570-9639/

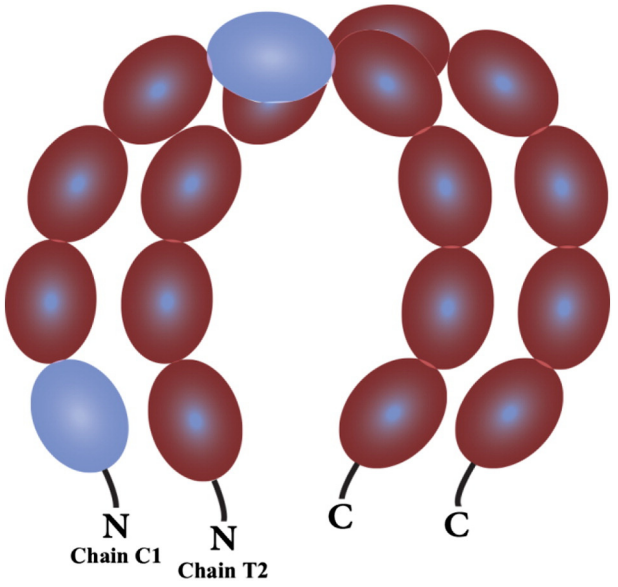

Fig. 1. Schematic view of *As*HbII. *As*HbC1D1 and *As*HbC1D5 are presented in blue.

and are presumed to be copied originally from a single-domain gene [11,14]. Phenotypically, two of these ring-shaped globin chains dimerize, by coaxially stacking, to produce three heterodimeric Hb isoforms (M_r ~320,000): HbI (C1C2), HbII (C1T2) and HbIII (T1T2) [12]. Analysis of the Hb quaternary structure demonstrates that in both globin chains the EF helices of all domains are in contact along the interpolymer surface, and that domain 1 of the T-polymer aligns with domain 1 of the C-polymer. Similar EF contacts are very common in cooperative Hbs [15].

The *Artemia* Hbs are definitively involved in O_2 storage/transport metabolism and serve e.g. to cope with the variable O_2 tension in the environment. All three Hbs bind O_2 cooperatively and with a different affinity [16]. Their biosynthesis is differentially controlled according to the species where they are expressed in, the ontogenetical stage and the temperature, pH and the O_2 tension of the habitat [10,17–20].

The role of the individual domains in the polymeric globin chain(s) and the native Hb(s) is unclear. However, single or multi-domain fragments of *Artemia salina* (*As*HbII), obtained by limited proteolysis, bind O_2 non-cooperatively [21,22].

This paper aims to answer the following questions; firstly, whether the eighteen domains have the same role in the ligand binding or not; secondly, whether the general structure of the heme pocket in the native Hb of *Artemia* is the same as that of myoglobin, and finally, whether Hb of *Artemia*, with 18 heme centers, has a higher redox potential than the normal reference globins.

To provide an answer to these questions, we studied the physicochemical characteristics (electron paramagnetic resonance (EPR), laser-flash photolysis and redox chemistry) of two recombinant globin domains [*A. salina* chain C1, domains 1 (*As*HbC1D1) and 5 (*As*HbC1D5) (Fig. 1)] of *Artemia urmiana* and *Artemia franciscana* from Urmia salt Lake, Iran and compared them with those of native Hbs of *A. franciscana* (*Af*Hb).

2. Materials and methods

2.1. Purification of *A. franciscana* Hbs (*Af*Hb)

Native *A. franciscana* Hbs were purified from frozen material (a gift from the Laboratory of Aquaculture and *Artemia* Reference Center, University of Ghent, Belgium) mainly as described previously [23]. Shortly, crude *Af*Hb (50% ammonium sulfate precipitate) was further purified on a HiTrap DEAE column by step elution at 225 mM NaCl. Hb tracing was spectrophotometric at 412 nm.

2.2. RNA extraction and amplification

A. urmiana and *A. franciscana* were collected from Urmia Salt Lake, Urmia, Iran. Total RNA was prepared using the combination of TriZol method and PureLink RNA Mini Kit. cDNA was synthesized as described elsewhere [24]. The cDNA fragments encoding globin domains 1 (*As*HbC1D1) and 5 (*As*HbC1D5) of chain C1 were amplified by PCR [25].

2.3. Cloning, expression, and purification of recombinant proteins

The PCR products were cloned into the TOPO-TA vector (Invitrogen) followed by subcloning into pET23a vector. *As*HbC1D1 and *As*HbC1D5 were expressed in *Escherichia coli* strain BL21(DE3)pLysS. Cells were grown at 37 °C in Terrific Broth (TB) medium (1.2% bactotryptone, 2.4% yeast extract, 0.4% glycerol, 72 mM potassium phosphate buffer, pH 7.5) containing 200 μg/ml ampicillin, 30 μg/ml chloramphenicol, and 2.5 mM δ-amino-levulinic acid. The culture was induced at $A_{550} = 1.2$ by the addition of isopropyl-1-thio-β-D-galactopyranoside (IPTG) to a final concentration of 0.4 mM, and expression was continued overnight (at 25 °C). The cells were harvested and resuspended in lysis buffer, 50 mM Tris–HCl (pH 7.5) containing 300 mM NaCl.

The cells were exposed to three freeze–thaw steps and sonication till completely lysed. The lysate was clarified by low speed (10 min at 10,000 ×*g*) centrifugation. Then, imidazole was added (final buffer composition of 50 mM Tris–HCl pH 7.5, 300 mM NaCl, and 20 mM imidazole) and the extract loaded on a Ni-affinity His 60 super flow column (Clontech), equilibrated with the same buffer. After washing of the unbound material, the His-tagged recombinant protein was eluted by 50 mM Tris–HCl pH 7.5, 300 mM NaCl and 500 mM imidazole. The fractions containing the proteins of interest were pooled and dialyzed against 50 mM Tris–HCl pH 7.5 containing 150 mM NaCl and 0.5 mM EDTA. After concentration by ultra-filtration (Amicon PM 10), the samples were loaded on Superdex Gf75, 15 × 1800 tricorn column (GE Healthcare) for gel filtration chromatography. All purification steps were assessed by SDS-PAGE.

2.4. UV–visible spectroscopy

Optical measurements were done with a Varian Cary-5 UV–visible near-infrared spectrophotometer (Varian, Palo Alto, California). All UV–visible spectra were measured in the range from 250 to 700 nm.

2.5. Continuous wave EPR of the native protein

X-band continuous wave (CW) EPR measurements were performed on a Bruker ESP300E spectrometer with a microwave frequency of 9.45 GHz equipped with a gas-flow cryogenic system (Oxford Inc.), allowing for operation from room temperature down to 2.5 K. The magnetic field was measured with a Bruker ER035M NMR Gauss meter. During the experiments, a vacuum pump was attached to the EPR tube in order to remove O_2 from the frozen sample. The spectra are measured with modulation amplitude of 0.8 mT, a modulation frequency of 100 kHz and a microwave power of 0.1 mW.

For the EPR measurements, 20% glycerol was added as a cryoprotectant. All spectra were simulated using EasySpin, a toolbox for MATLAB (Mathworks, Natick, Mass., USA).

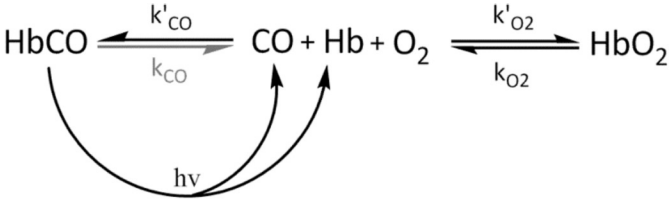

Scheme 1.

Please cite this article as: H.A. Borhani, et al., Kinetic properties and heme pocket structure of two domains of the polymeric hemoglobin of *Artemia* in comparison with the native molecule..., Biochim. Biophys. Acta (2015), http://dx.doi.org/10.1016/j.bbapap.2015.05.007

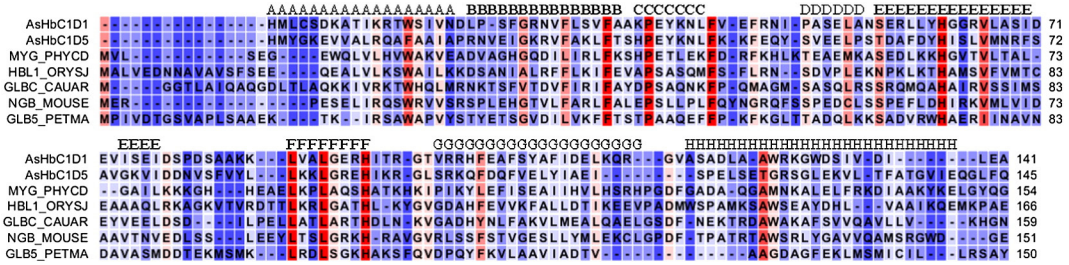

Fig. 2. Alignment of the *As*HbC1D1 and *As*HbC1D5 with reference hemoglobin/myoglobin. Reference molecules are the globin domains of sperm whale Mb (MYG_PHYCD, P02185), non-symbiotic Hb 1 of *Oryza sativa*, rice (HBL1_ORYSJ, O04986), globin C of *Caudina arenicola* (GLBC_CAUAR, P80018), mouse neuroglobin (NGB_MOUSE, Q9ER97) and globin 5 of *Petromyzon marinus* (GLB5_PETMA, P02208).

2.6. Analytical gel filtration experiments

The apparent M_r of the recombinant *As*HbC1D1 and *As*HbC1D5 in solution was assessed by analytical gel filtration experiments using a Superdex G27 (2 × 30 cm; buffer 50 mM Tris–HCl pH 7.5, 150 mM NaCl and 0.5 mM EDTA; 0.5 ml·min^{-1}) calibrated with human Hb (68 kD), cytoglobin (42 kD) and myoglobin (17 kD). Protein elution was monitored at 280 and 412 nm. Concentration dependent oligomerization was tested by loading different Hb concentrations (3.3 μM, 11.1 μM, 42.5 μM and 85.1 μM).

2.7. O_2 equilibria

The O_2 equilibrium curve for *Af*Hb was determined using a modified diffusion chamber technique described previously [26,27]. Shortly, water-saturated gaseous mixtures of O_2 and ultrapure (>99.998%) N_2 created by Wösthoff (Bochum, Germany) gas mixing pumps were used to equilibrate a thin smear (190 μM heme) of the *Af*Hb solution with different values of O_2 tension (P_{O_2}). Changes in absorbance upon oxygenation were recorded continuously at 436 nm by a photomultiplier (model RCA 931-A, Hamamatsu, Hamamatsu city, Japan) and an Eppendorf model 1100 M photometer (Hamburg, Germany) coupled to a potentiometric linear recorder. For reference, 0 and 100% O_2 saturation levels were obtained by equilibrating with pure N_2 and O_2, respectively, at the beginning and end of the experiment. P_{50} (P_{O_2} at half-saturation) and n_{50} (cooperativity) values were calculated from the zero intercept and slope, respectively, of Hill plots: log [Y / (1 − Y)] versus log P_{O_2}, where Y is the fractional saturation of Hb. The curve consists of four to five saturation steps. Experiments were carried out in duplicate in 100 mM potassium phosphate, pH 7.0 at 20 °C.

2.8. Ligand-binding kinetics

2.8.1. CO binding kinetics

To measure the rates of CO association, the Fe^{3+} Hb stock solution was diluted with a 100 mM potassium phosphate buffer, 1 mM EDTA, pH 7.0, at 20 °C to a final concentration of ~5 μM, equilibrated in different concentration (200–800 μM) of CO and anaerobically reduced with 1 mM sodium dithionite. The experimental setup was described in detail elsewhere [28,29]. Shortly, photolysis of HbCO samples was carried out on a laser photolysis system (Edinburg Instrument LP920) at 20 °C using the second harmonic (532 nm) of a frequency-doubled Q-switched Nd:YAG laser (Spectra Physics Quanta-Ray). The absorbance changes were recorded with a Tektronix TDS220 digitizing oscilloscope fitted to a simple exponential expression. CO association rate value (k'_{CO}) was calculated as the slope of plots of k_{obs} versus [CO]. For all ligand-binding kinetic studies, measurements were done at least in triplicate and averaged.

2.8.2. Geminate recombination

The geminate rebinding time courses were fitted to one exponential decay. The observed rates of geminate rebinding (k_{gem}) were independent of ligand concentration. The fraction of geminate recombination (F_{gem}) was calculated using Eq. (1):

$$F_{gem} = \Delta A_{gem}/\Delta A_{gem} + y_0 \quad (1)$$

where ΔA_{gem} represents the absorbance change associated with the internal geminate rebinding and y_0 (the offset) is the difference between the absorbance after complete geminate recombination and the absorbance of the original ground state, which is observed prior to the photolysis or at the long times after the complete rebinding of bimolecular from the solvent. As the concluded rates for CO entry and exit appeared to be the

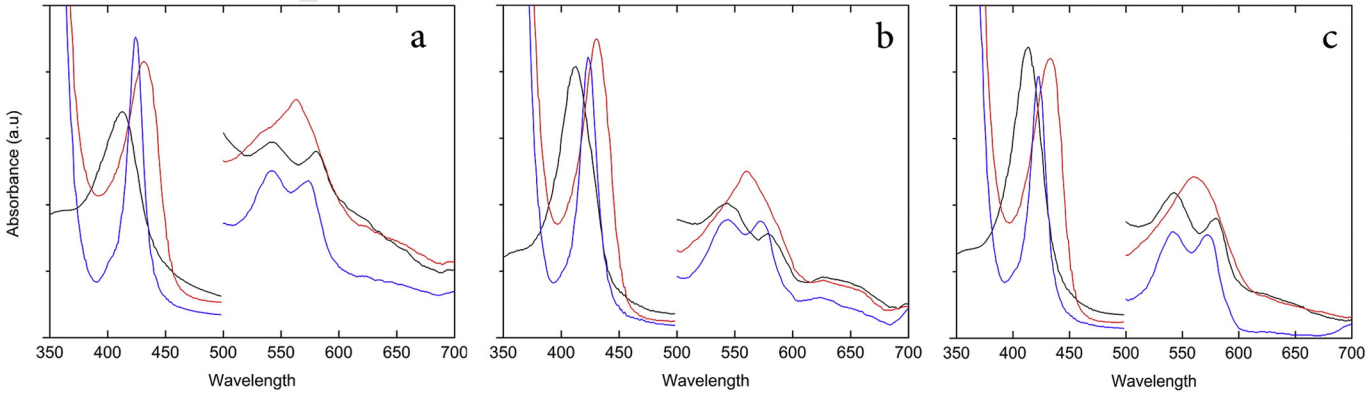

Fig. 3. Absorption spectra of *As*HbC1D1 (a), *As*HbC1D5 (b) and *Af*Hb (c). As purified-oxygenated form (black line), dithionite-reduced Fe^{2+} deoxygenated form (red line) and the carbonylated form (blue line).

same for those of O_2 and NO due to the almost same size and polarity of three diatomic gases [30], the geminate rebinding parameters were measured for CO.

2.8.3. O_2 binding kinetics

Time courses for O_2 association and dissociation were measured after complete laser photolysis of Hb samples containing various mixtures of O_2/CO. The mixed atmosphere allows measurement of the O_2 dissociation rate. In these experiments, Hb samples were prepared in five different buffers with 100 mM potassium phosphate buffer, pH 7.0, at 20 °C containing various concentration of CO and O_2 (e.g. 892 μM of CO, 750 μM of CO and 312.5 μM of O_2, 500 μM of CO and 625 μM of O_2, 250 μM of CO and 937.5 μM of O_2, and 1250 μM of O_2). The sample is essentially bound to CO at equilibrium because the partition coefficient between both ligands is displaced toward the CO form as occurs for most globins.

As shown in Scheme 1, the photolysis of HbCO by a laser beam generates a deoxyHb species which react rapidly with either ligand and two distinct phases were observed. The rate of bimolecular rebinding phase (k_{fast}) that was dominated by O_2 rebinding due to its larger association constant (k'_{O_2}), was monitored by a large decrease in the absorbance of unliganded Hb at 436 nm [31]. The value of k_{fast} is given by Eq. (2),

$$k_{fast} = k'_{O_2}[O_2] + k_{O_2} + k'_{CO}[CO]. \quad (2)$$

Generally, the CO dissociation occurs on a timescale slower compared to the O_2 and then can be treated as an irreversible process.

The slow replacement phase represents the displacement of transiently bound O_2 by CO, which, although kinetically less reactive, has a higher affinity for heme. The time course of this replacement reaction is best monitored by a large increase in the difference of absorbance at 422–424 nm. The rate of this process, k_{slow}, is given by Eq. (3),

$$k_{slow} = \frac{k_{O_2}}{1 + \dfrac{k'_{O_2}[O_2]}{k'_{CO}[CO]}}. \quad (3)$$

An iterative, nonlinear, least squares fitting routine (Solver in Microsoft Excel) was used to optimize the values of k'_{O_2}, k_{O_2}, and k'_{CO} to give the best fit to the dependence of k_{fast} and k_{slow} on $[O_2]/[CO]$, including conditions of $[O_2] = 0$ and $[CO] \approx 0$ [31].

2.9. Reduction potential

Electrochemical measurements were conducted in a conventional three-electrode cell using a μAutolab III interface controlled by Nova 1.10 software (Metrohm-Autolab BV, Netherlands). A saturated calomel electrode (SCE, 0.248 V versus standard hydrogen electrode (SHE) at 20 °C) and a glassy carbon rod were used as the reference and auxiliary electrodes, respectively. Prior to modification, the gold electrodes (1.6 mm in diameter, BASi, USA) were polished with 1 and 0.05 μm alumina slurry, washed, and sonicated in ultrapure water for about 5 min. Next, the electrodes were electrochemically cleaned by cyclic voltammetry (CV) in 0.5 M NaOH at the potential range from −0.35 to −1.35 V and in 0.5 M H_2SO_4 at the potential range from 0.2 to 1.5 V vs. SCE until repeatable cyclic voltammograms. Then, the electrodes were incubated overnight in 10 mM 6-mercapto-1-hexanol (97%, Sigma-Aldrich) solution in water. Finally, the electrodes were thoroughly washed with water and dried in air stream. Electrochemistry of the proteins was studied using membrane electrodes as described [32,33]. Briefly, 2–3 μl of a protein solution was entrapped between the electrode and dialysis membrane (MWCO 12 kD). Differential pulse voltammetry (DPV) was recorded before and after placing the samples on the electrodes.

Table 1
The absorption maxima of *As*HbC1D1, *As*HbC1D5 and *Af*Hb in different forms.

	Soret band (nm)	β-Band (nm)	α-Band (nm)
As purified oxy-form			
*As*HbC1D1	413	540	579
*As*HbC1D5	412	544	579
*Af*Hb	413	540	582
Reduced deoxy-form			
*As*HbC1D1	431	Shoulder 528	562
*As*HbC1D5	431		559
*Af*Hb	433		563
Carbon monoxy-form			
*As*HbC1D1	424	544	573
*As*HbC1D5	423	545	571
*Af*Hb	423	540	572

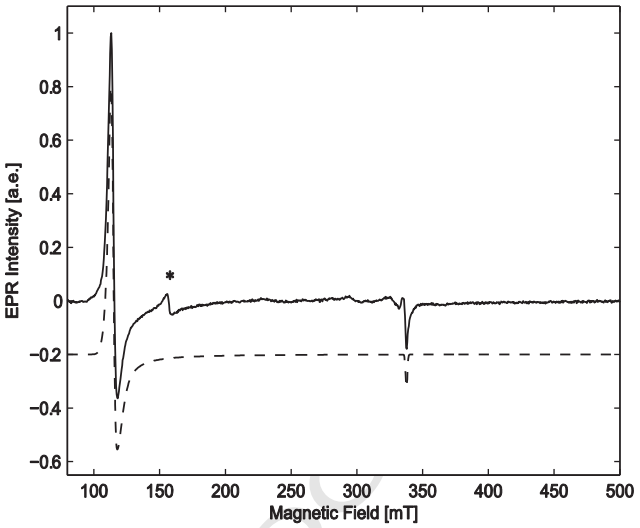

Fig. 4. X-band CW-EPR spectra of ferric native *Af*Hb (solid) and simulation (dashed). The asterisk shows the contribution to the signal of non-heme iron. All spectra were recorded at 10 K.

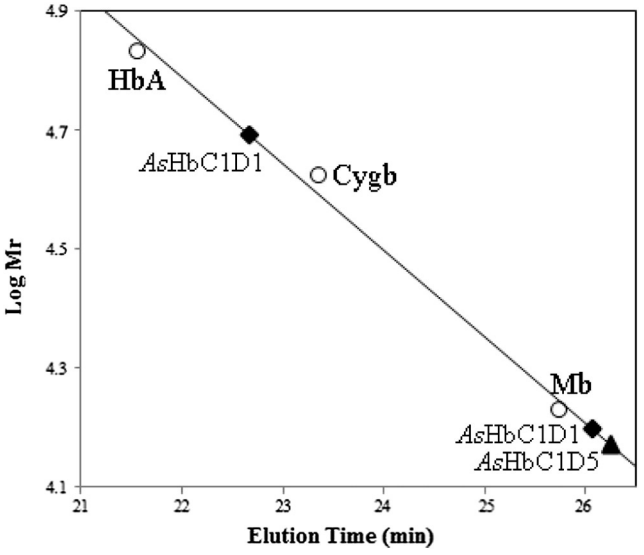

Fig. 5. Analytical gel filtration experiments. Dependence of the molecular mass on elution time; the globin standards (open circles) were human hemoglobin (HbA), human cytoglobin (Cygb), horse heart myoglobin (Mb) along with *As*HbC1D1 (♦) and *As*HbC1D5 (▲).

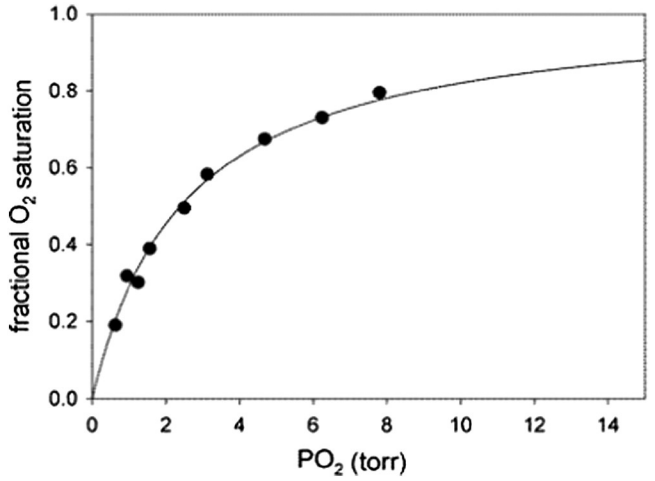

Fig. 6. Oxygen binding equilibrium curve for *Af*Hb.

3. Results

3.1. Cloning, expression and purification

The obtained cDNA sequences for domains 1 and 5 from both species were compared with the reported sequence of *Artemia* by Manning et al. [10]. For cDNA sequences of domain 1 from *A. urmiana* and *A. franciscana* two differences (positions 102 and 393) and for that of domain 5 one difference (position 391) were noted. The corresponding protein sequences for both domains were exactly the same as reported in literature. Therefore, *As*HbC1D1 and *As*HbC1D5 were used as abbreviations to refer to the recombinant proteins of both species. *As*HbC1D1 and *As*HbC1D5 are composed of 141 and 145 residues, respectively. The primary structure comparison indicated 26.1% identity and 41.8% similarity between the domains. Moreover, *As*HbC1D1 sequence is more similar to the non-symbiotic Hb1 of *Oryza sativa*, rice (38.8%) and to the globin C of *Caudina arenicola* (41.0%) whereas *As*HbC1D5 is similar to the mouse neuroglobin (40.6%) and the globin 5 of *Petromyzon marinus*, sea lamprey (39.1%) (Fig. 2). Expression and purification of the recombinant *As*HbC1D1 and *As*HbC1D5 yielded two recombinant proteins with a molecular mass ~16–17 kD, as verified by SDS-PAGE and gel filtration. The recombinant proteins were, however, not that stable and hard to store. *Af*Hb was successfully purified from the brine shrimp and showed a molecular mass of 160 kD by SDS-PAGE.

3.2. UV–visible spectroscopy

Fig. 3 shows the UV–visible absorption spectra of expressed/purified species of *As*HbC1D1, *As*HbC1D5 and *Af*Hb in the oxy-, deoxy- and carbon monoxy-forms. The optical absorption spectra of the oxy-form of *As*HbC1D1 and *As*HbC1D5 show the Soret maximum at 412 nm and α and β maxima at 579 nm and 540 nm, respectively (Fig. 3, Table 1). This is a typical absorbance spectrum for oxygenated globins, such as sperm whale myoglobin. Moreover, the absorption spectrum of the freshly purified *Af*Hb exhibits the Soret maximum at 413 nm and α and β maxima at 579 nm and 540 nm, respectively.

Upon CO binding to ferrous *As*HbC1D1, *As*HbC1D5 and *Af*Hb, the Soret maxima are shifted to 424, 423 and 423 nm, respectively. The α and β maxima are observed at 571–573 nm and 540–545 nm (Table 1).

3.3. Continuous wave EPR of the native Hb

The EPR spectrum of ferric native *Af*Hb is shown in Fig. 4 and indicates that the system is in a high-spin (HS) state. In this state, the distal side of the central heme iron is known to bind weak ligands like H_2O or have no distal ligand. Simulation of this spectrum gives the following *g*-values: $g_x = 5.92$, $g_y = 5.91$ and $g_z = 1.996$. After addition of imidazole (1:1 ratio imidazole:heme), which is a strong base, we expect imidazole to bind to the distal side of the heme iron because of the competition with the weak ligand, as is reported for metmyoglobin [34]. The EPR spectrum after addition of imidazole however shows no appearance of a low-spin state typical for an imidazole-ligated globin. This indicates that the imidazole is not able to enter the heme-pocket, and thus native *Af*Hb has a more closed heme-pocket structure than myoglobin.

3.4. Oligomerization state analysis by gel filtration

Analytical gel filtration experiments were performed to assess the quaternary structure of *As*HbC1D1 and *As*HbC1D5 in solution (expected molecular mass = 16.5 and 17.2 kD, respectively, as calculated from sequence analysis). Elution time for *As*HbC1D1 (Fig. 5) corresponds to two peaks with molecular mass around 50 kD and 16 kD, values consistent with a tetramer and a monomer assembly, respectively. The elution time for *As*HbC1D5 correspond to a molecular mass of 15 kD, which indicates a monomeric structure (Fig. 5). The elution times for both proteins were the same for all tested concentrations, which indicates that the oligomerization of both proteins is independent of protein concentration.

3.5. O_2 equilibria

*Af*Hb O_2 binding curve was hyperbolic (Fig. 6) with a P_{50} value of 2.46 Torr, while the reported P_{50} values for *Artemia* Hb I, Hb II and Hb III were 5.34, 3.70 and 1.80 mm Hg, respectively [17]. Moreover, the calculated P_{50} value based on the association constant of O_2, K^{O_2}, was 1.51 Torr (Table 3). The difference can be explained by the different experimental conditions (e.g. pH and temperature). The native Hb showed a cooperativity value (n_{50}) close to 1.04, which is different from the

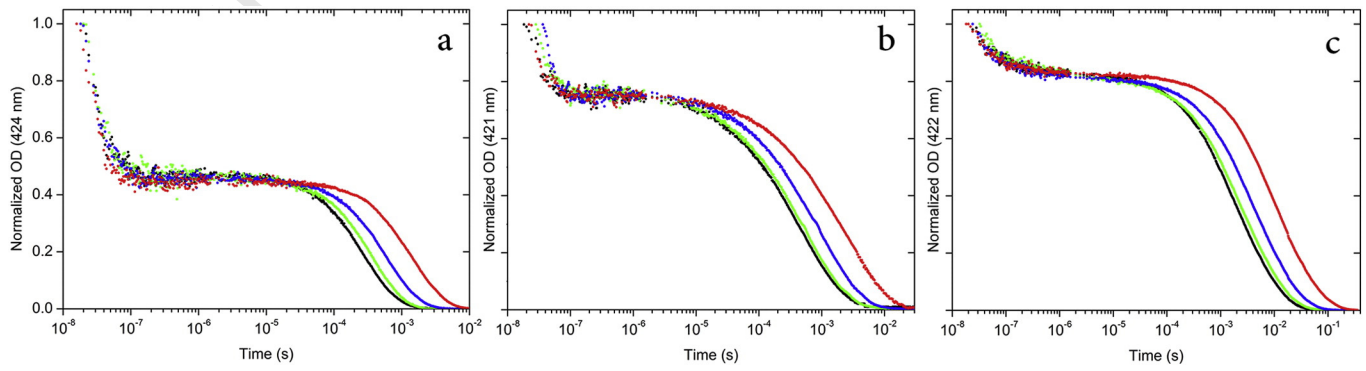

Fig. 7. CO rebinding after nanosecond laser photolysis. CO rebinding kinetics to *As*HbC1D1 (a), *As*HbC1D5 (b) and *Af*Hb (c) solution at 20 °C (black, 1000 μM CO; green, 800 μM CO; blue, 400 μM CO; red, 200 μM CO).

Table 2
Kinetic values for O_2 and CO reactions of *As*HbC1D1, *As*HbC1D5 and *Af*Hb at pH 7, 20 °C with some selected hemoglobin/myoglobin.

	k'_{O_2}	k_{O_2}	K_{O_2}	P_{50}, Torr	k'_{CO}	k_{gem}	F_{gem}	k_{bond}	k_{escape}	k'_{entry}	Ref.
	$\mu M^{-1}\ s^{-1}$	s^{-1}	μM^{-1}		$\mu M^{-1}\ s^{-1}$	μs^{-1}		μs^{-1}	μs^{-1}	$\mu M^{-1}\ s^{-1}$	
*As*HbC1D1	10.5 ± 1.6	8.1 ± 0.8	1.30 ± 0.18	0.42[a]	3.32 ± 0.18	55 ± 3	0.57 ± 0.01	31.35 ± 3	23.65 ± 4.2	5.82 ± 0.18	This work
*As*HbC1D5	13.2 ± 1.2	15.3 ± 2.1	0.86 ± 0.05	0.64[a]	15.9 ± 1.6 1.3 ± 0.05	61 ± 0.7	0.23 ± 0.01	14.03 ± 0.7	46.97 ± 1	69.13 ± 1.6 5.65 ± 0.05	This work
*Af*Hb	8.1 ± 0.7	35.4 ± 4.9	0.23 ± 0.05	2.39[a] (2.46[b])	1.7 ± 0.35 0.17 ± 0.02	17 ± 0.6	0.19 ± 0.01	3.23 ± 0.6	13.77 ± 0.84	8.95 ± 0.35 1.05 ± 0.02	This work
Carp Mb1	7.1	14.9	0.48	1	3.2, 0.9	11					[26]
Carp Mb2	16.6	75.2	0.22	1.7	4.4, 2.0	5					[26]
Hb α	32	13	2.6		5.2	24	0.14	3.4	21	36	[30]
Hb β	82	28	3.1		9.2	7.6	0.22	21.7	6	42	[30]
SWMb	16	14	1.14	0.9 [c]	0.7	12.12[d]	0.47 [d]	5.7[d]	6.3[d]	34[d]	[35–37]
CerHb[e]	230	190	1.2		32	80	0.05	4	76	640	[38]
Chironomus Hb	300	218	1.37		0.27						[39]

[a] These values are calculated based on K_{O_2} values (i.e. $P_{50} = 1/(1.82 * K_{O_2})$).
[b] P_{50} value was measured by O_2 equilibrium.
[c] Calculated in 22 °C.
[d] The kinetic values are measured based on O_2 as ligand, whereas those of the recombinant proteins are measured based on CO.
[e] *Cerebratulus lacteus* mini-hemoglobin.

value of the previous report by D'Hondt study [17]. However, they reported the n_{50} value for each type of *Artemia*'s Hb.

3.6. Ligand binding kinetics

3.6.1. CO association rate constant

The CO association rates of *As*HbC1D1, *As*HbC1D5 and *Af*Hb were measured using Laser Flash Photolysis. Fig. 7 reports the fraction of deoxy heme as a function of time after the photolysis for selected conditions. Two distinct processes in the CO rebinding curves are clear: i) A fast rebinding phase or geminate rebinding, which was completed in less than 2000 ns, and shows no dependence on CO concentration; and ii) a slower phase, whose apparent rate constant depends on CO concentration, and is called bimolecular rebinding. The latter indicates the rebinding of ligands to heme iron from the solvent phase.

As shown in Fig. 7, the ligand recombination in *As*HbC1D1 and *As*HbC1D5 is remarkably different from each other. *As*HbC1D1, showed monophasic kinetics and the extracted association rate constant is 3.32 μM^{-1} (Table 2). Furthermore, *As*HbC1D1 has slightly higher association rate constant than *As*HbC1D5, suggesting a greater accessibility of this domain for CO. CO bimolecular rebinding of both *As*HbC1D5 and *Af*Hb, however, shows biphasic kinetics that could be fitted by a double exponential relaxation. Therefore, as indicated in Table 3, the bimolecular CO association rate constants of *As*HbC1D5 are 15.9 and 1.3 μM^{-1}, and that of *Af*Hb are 1.7 and 0.17 μM^{-1}. This kinetic heterogeneity for *As*HbC1D5 and *Af*Hb suggests the existence of two different conformations at equilibrium. Moreover, it is noteworthy to mention that, as there are 18 globin domains in AfHb, we cannot make a distinction between the rates of the separate domains when measuring on the native Hb.

3.6.2. Geminate rebinding parameters

Internal CO geminate recombination was examined on nanosecond time scales to first determine the fraction of geminate recombination (F_{gem}) and secondly to estimate rates of internal ligand bond formation and escape. The F_{gem} values of the two recombinant proteins are 0.57 and 0.23, respectively, which indicate a different heme pocket structure or a different escape route in these proteins. The F_{gem} value of *Af*Hb is more close to the value of *As*HbC1D5 (i.e. 0.19) (Fig. 8, Table 2).

The above mentioned kinetic features are shared with sperm whale Mb (SWMb) [35], although there are some small variations in the relative extent of the different phases. In particular, the fraction of geminate recombination for *As*HbC1D1 (0.57) is higher than that of SWMb (0.47), whereas F_{gem} of *As*HbC1D5 (0.23) is lower than that of SWMb (Table 2). However, it should be noted that the F_{gem} and other kinetic values of SWMb in [35] were measured based on O_2 as ligand.

As shown in Fig. 8, the geminate CO recombination in all three samples appears to be a simple first order process. The k_{gem} values of *As*HbC1D1, *As*HbC1D5 are close (i.e. 55 and 61 μs^{-1}, respectively) which is nearly 4 times greater than that of *Af*Hb (i.e. 17 μs^{-1}) (Table 2).

The bimolecular and geminate recombination parameters could be used in calculating the internal binding and escaping rates of ligand to or from the inside of the protein.

A two-step binding scheme was assumed for analysis that involved internal bond formation between the ligand and iron atom (k_{bond}) and for ligand escape (k_{escape}) from or bimolecular return (k'_{entry}) to the geminate state (Hb···CO) in Scheme 2 [30]. The rate parameters which fit to these processes, define the observed rates (k_{gem}, Eq. (5)) and the fractions (F_{gem}, Eq. (4)) of geminate recombination and the overall bimolecular CO association rate constant (k'_{CO}, Eq. (6)) [30,40]:

$$F_{gem} = \frac{k_{bond}}{k_{bond} + k_{escape}} \quad (4)$$

$$k_{gem} = k_{bond} + k_{escape} \quad (5)$$

$$k'_{CO} = \frac{k'_{entry} k_{bond}}{k_{escape} + k_{bond}} = k'_{entry} F_{gem}. \quad (6)$$

The rate constant for the ligand entry, k'_{entry}, into the individual proteins is calculated empirically as the observed bimolecular rate constant divided by the fraction of geminate recombination ($k'_{entry} = k'_{CO} / F_{gem}$). Therefore, k'_{entry} is calculated independently [30,40].

The values of internal binding, ligand entry and escaping parameters for studied proteins are listed in Table 3. As it is clear from Table 3, the k_{bond} values for *As*HbC1D1, *As*HbC1D5 and *Af*Hb are 31.35, 14.03 and 3.23 μs^{-1}, respectively, while the k_{escape} values are 23.65, 46.27 and 13.77 μs^{-1}, respectively. It must be noted that the k'_{entry} for *As*HbC1D1

Table 3
Reduction potential of *Af*Hb, *As*HbC1D1 and *As*HbC1D5 based on the differential pulse voltammograms.

	Ep, reduction (V vs. SCE)	$E_{1/2}$ (V vs. SCE)[a]	$E_{1/2}$ (V vs. SHE)[b]
*Af*Hb	−0.361 ± 0.005	−0.374 ± 0.005	−0.126 ± 0.005
*As*HbC1D1	−0.399 ± 0.005	−0.412 ± 0.005	−0.164 ± 0.005
*As*HbC1D5	−0.426 ± 0.005	−0.439 ± 0.005	−0.191 ± 0.005

[a] $E_{1/2} = E_{peak} + E_{modul} / 2$.
[b] Potential of SCE is +0.248 V vs. SHE at +20 °C.

Please cite this article as: H.A. Borhani, et al., Kinetic properties and heme pocket structure of two domains of the polymeric hemoglobin of *Artemia* in comparison with the native molecule..., Biochim. Biophys. Acta (2015), http://dx.doi.org/10.1016/j.bbapap.2015.05.007

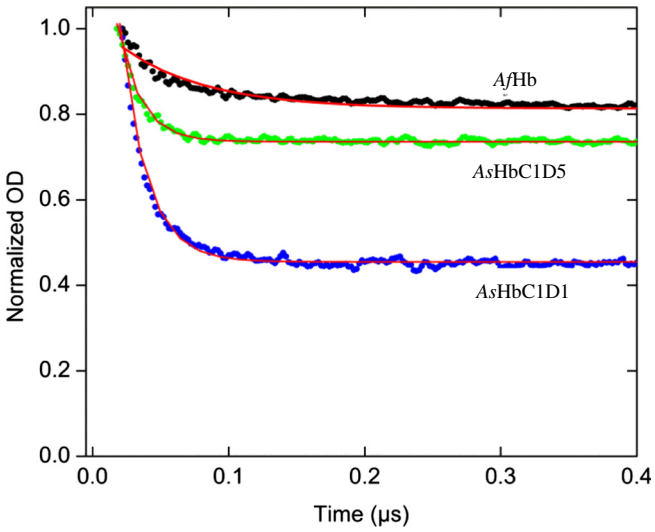

Fig. 8. Time course of CO geminate rebinding to *Af*Hb, *As*HbC1D1 and *As*HbC1D5.

is 5.82 $\mu M^{-1}\ s^{-1}$, whereas this parameter for *As*HbC1D5 and *Af*Hb has two values (see Table 2).

3.6.3. O_2 association and dissociation rate constant

Table 3 summarizes the kinetic properties of recombinant and native *Artemia* proteins in comparison with those of some reference Hb/Mb. O_2 association rate constants for *As*HbC1D1, *As*HbC1D5 and *Af*Hb are 10.5, 13.2 and 8.1 $\mu M^{-1}\ s^{-1}$, respectively. Although the association rate constants are very similar for all different proteins, the O_2 dissociation rate constants are not. Indeed the *As*HbC1D5 domain has a higher k_{O_2} (15.3 s^{-1}) whereas it is even higher for *Af*Hb (35.4 s^{-1}). The O_2 dissociation rate constants of *As*HbC1D5 and *Af*Hb are respectively a factor of 2 and 4 higher, which makes the affinity for O_2 for these two proteins lower.

Calculated P_{50} values of *As*HbC1D1 and *As*HbC1D5 are 0.42 and 0.64 Torr, respectively. The calculated P_{50} for the native protein is 2.39 Torr, which is very close to the measured P_{50} by O_2 equilibria (2.46 Torr). Therefore, the P_{50} value for native Hb is significantly higher and O_2 affinity is lower in comparison with the recombinantly expressed domains. O_2 binding constant of *As*HbC1D1 (1.30 μM^{-1}) is similar to *Chironomus thummi thummi* Hb [39] and the values of *As*HbC1D5 (0.86 μM^{-1}) is more like to Mb2 of carp [26] (Table 2)

3.7. Reduction potential

Fig. 9 shows differential pulse voltammograms of the native and recombinant proteins. The redox potential is found from the peak position and differs noticeably among the proteins. As shown in Table 4, *Af*Hb has the highest reduction potential $E_{1/2}$ (−0.13 V versus SHE) compared to *As*HbC1D1 (−0.16 V) and *As*HbC1D5 (−0.19 V).

4. Discussion

This present study was conducted to examine the role of the different domains in ligand binding of *Artemia* Hb by comparing the characteristics of the isolated domains to the native molecule. By cloning and expressing the two individual domains (*As*HbC1D1: a N-terminal located domain; and *As*HbC1D5: an internally located domain) separately, we have created one-domain, single-heme globin-like proteins, which mediate ligand binding.

When comparing the C1D1 domain of *A. franciscana* and *A. urmiana* there is no difference in the sequence at the protein level (Fig. 2) and only few differences at the DNA level. The same conclusion can be taken for the C1D5 domain. This suggest that strain specific sequence differences are negligible.

Although there is a low identity between both recombinant domains and SWMb (~25%) virtually all key hydrophobic and heme-binding residues are conserved suggesting that both domains display the genuine globin fold (Fig. 2). A first indication that confirms this, is the UV–Vis spectroscopy, which shows that both recombinant domains as well as the native *AfHb*, are pentacoordinated like SWMb (Fig. 3). EPR spectroscopy, however, demonstrates that ferric native *AfHb* is unable to bind imidazole into the heme pocket suggesting a more closed structure than seen in SWMb (Fig. 4).

The quaternary structure of both recombinant globin domains in solution was studied by gel filtration experiments. They show that *As*HbC1D1 occurs predominantly as tetramer and monomer whereas *As*HbC1D5 occurs only as monomer. This suggests that the function of both domains in the assembly of the native *As*Hb molecule is different (Fig. 5). Furthermore as each globin domain separately is not stable in physiological buffers, the polymeric structure is essential to stabilize the Hb structure in *Artemia*. Hence, this confirms that the concatenation of globin domains into polymeric globin chains, as mentioned by Weber et al., is indispensable for stability [7].

The ligand binding kinetics and equilibrium studies of the native *Af*Hb and the recombinant domains C1D1 and C1D5 also indicate slight differences in properties. The P_{50} value of 2.46 Torr obtained by equilibrium measurements is very close to the P_{50} calculated from the kinetic rate constants (2.39 Torr). They are, however, different from the published values (17) probably due to the fact that the *Af*Hb we used is a mixture of the three Hb types and the difference in the experimental conditions (e.g. pH and temperature) used (Fig. 6; Table 3). Calculated P_{50} values of *As*HbC1D1 and *As*HbC1D5 were 0.42 and 0.64 Torr, respectively. The difference in O_2 affinity is due to a 1.88-fold higher O_2 dissociation rate constant (k_{O_2}) of *As*HbC1D5 compared to *As*HbC1D1, whereas the O_2 association rate constant (k'_{O_2}) of *As*HbC1D5 is only 1.25-fold higher than *As*HbC1D1 (Tables 2, 4). Furthermore, the O_2 association equilibrium constant of the native protein is lower than both

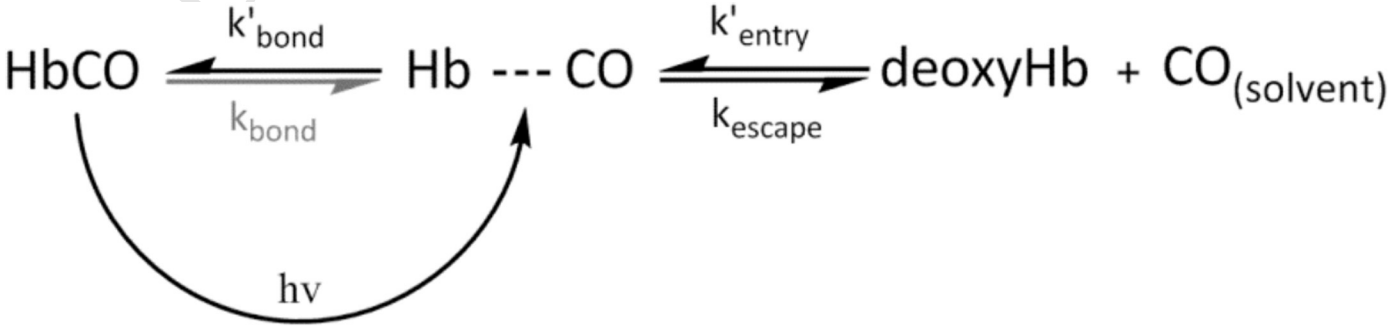

Q2 **Scheme 2.**

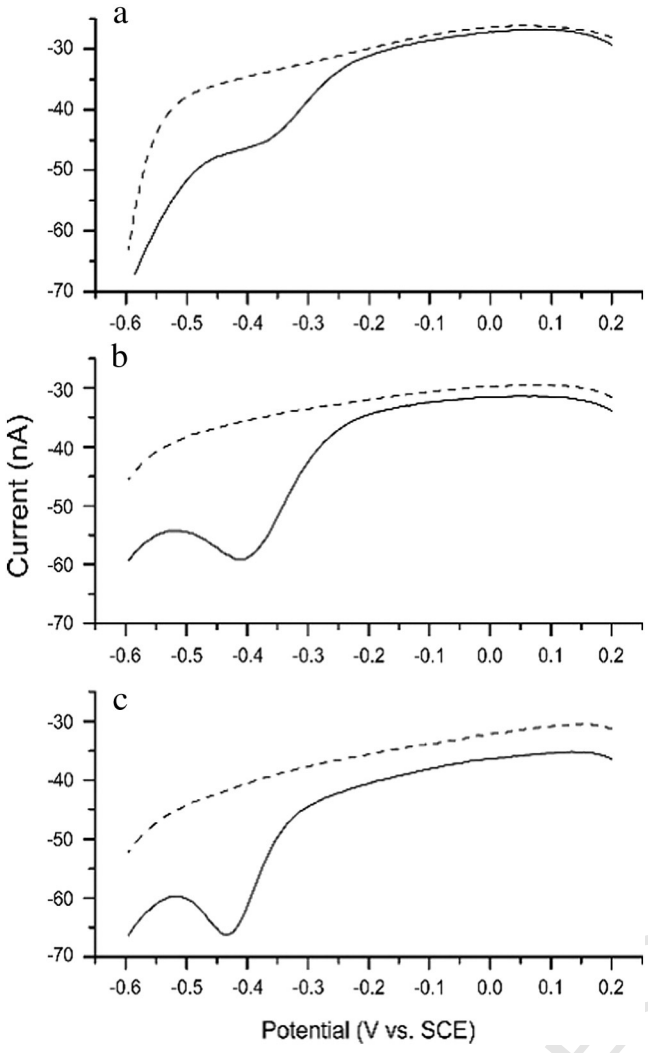

Fig. 9. Differential pulse voltammograms of *Af*Hb (a), *As*HbC1D1 (b) and *As*HbC1D5 (c). Broken lines show background of the electrodes recorded before placing the proteins. $E_{modul} = -25$ mV, $E_{step} = -5$ mV; $t_{modul} = 50$ ms, $t_{step} = 0.5$ s. Measuring buffer was 10 mM HEPES (pH 7) containing 0.1 M NaCl.

domains $\left(K_{O_2} = 0.23\ \mu M^{-1}\right)$ resulting mostly again from a higher dissociation rate constant ($k_{O_2} = 35.42\ s^{-1}$). Therefore, the P_{50} value for native *Af*Hb is significantly higher and thus O_2 affinity lower in comparison with the recombinant expressed domains. Nonetheless, the calculated and measured oxygen affinity is moderate and in the range of that of Mb.

When comparing the CO-ligand binding properties of the recombinant domains we see differences between themselves as well as with the native *As*Hb molecule. Indeed *As*HbC1D1 shows monophasic CO binding kinetics, while *As*HbC1D5 shows a double exponential relaxation. This points to a heterogeneity of the *As*HbC1D5 domain and may point to the existence of two conformations. It is noteworthy that the CO association rate of *As*HbC1D1 is 1.3-fold higher than *As*HbC1D5 (Table 2). Furthermore, from the geminate rebinding, we can conclude that there is a different fraction of geminate recombination for the proteins measured (Fig. 8).

Scott et al. studied the effect of point mutations in different positions of SWMb and compared the kinetic values of wild type and mutated proteins [35]. Some mutations in SWMb are in the same position as in *As*HbC1D1 or *As*HbC1D5 and are listed in Table 4. As an example, in position 65, the residue is Gly in SWMb and Ile in *As*HbC1D1. In Table 4, the kinetic values of mutation Gly to Ile in SWMb are compared with that of *As*HbC1D1. The comparison of the kinetic values of the recombinant domains with SWMb shows that K_{O_2} and F_{gem} of *As*HbC1D1 are more close to the wild type myoglobin than those of *As*HbC1D5. Mutation in the second shell of distal residue, such as Val66Gly (smaller residue) increases the F_{gem} from 0.47 to 0.58 which is finally similar to F_{gem} of *As*HbC1D1 (0.57). This also affects the K_{O_2} value and increases it from 1.14 to 1.79 μM^{-1} while the other mutation in this shell (Thr69Arg) does not vary the F_{gem}. Moreover, the point mutation Gly65Ile in the wild type SWMb, changes the K_{O_2} of SWMb (from 1.14 to 0.52 μM^{-1}) closer to the K_{O_2} of *As*HbC1D5 (0.86 μM^{-1}) while the F_{gem} does not change significantly (from 0.47 to 0.49). Hence, it shows that the position 65 may have a significant role in K_{O_2}. In other words, changing a small residue to a bigger one decreases the K_{O_2} value by 0.62 μM^{-1}. The other mutation in the distant place of heme such as Gln8Val modifies the K_{O_2} of SWMb from 1.14 to 0.49 μM^{-1} and closer to K_{O_2} of *As*HbC1D5 (0.86 μM^{-1}) (Table 4). It should be considered that as the tertiary structure of the domains is not available, the implementation of the functional and structural relationship may not be totally accurate.

Furthermore, as it was mentioned above, the value of k'_{entry} is defined experimentally as the rate constant for the ligand entry into the Hb. It is calculated as the observed bimolecular rate constant (k'_{CO}) divided by the observed total fraction of the internal rebinding (F_{gem}) (Eq. (6)). As it was also shown in Table 4, k'_{entry} for *As*HbC1D1 (5.84 $\mu M^{-1}\ s^{-1}$) is 6-times less than the value of SWMb, whereas the value for *As*HbC1D5 (69.13 $\mu M^{-1}\ s^{-1}$) is twice as big as the value of SWMb (34 $\mu M^{-1}\ s^{-1}$). This means that the two domains show variant ability for the ligand to enter the protein compared to SWMb. The rate of ligand entry in the *As*HbC1D5 is higher than that in the SWMb and shows that the ligand can more easily enter the heme pocket of the domains. The lower k'_{entry} of the native *Af*Hb confirms the closer heme-pocket structure seen using EPR. It must be noted that the values for SWMb are measured based on O_2 as the ligand, whereas we have used CO as ligand.

Table 4
Kinetic values[a] of *As*HbC1D1 and *As*HbC1D5 in comparison with wild type SWMb and its some point mutants based on [35].

	k'_{O_2}	k_{O_2}	K_{O_2}	k_{gem}	F_{gem}	k_{bond}	k_{escape}	k'_{entry}	Common with	Position of the mutation
	$\mu M^{-1}\ s^{-1}$	s^{-1}	μM^{-1}	μs^{-1}		μs^{-1}	μs^{-1}	$\mu M^{-1}\ s^{-1}$		
SWMb WT	16	14	1.14	12.12	0.47	5.7	6.3	34		
*As*HbC1D1	10.5 ± 1.6	8.1 ± 0.8	1.30 ± 0.18	55 ± 0.07	0.57 ± 0.01	31.35 ± 3	23.65 ± 4.2	5.82 ± 0.18		
V66G	25	14	1.79	27.8	0.58	14	9.8	43	*As*HbC1D1	Second Shell of distal Residue
T69R	12	11	1.08	13.3	0.47	6.3	7.0	26	*As*HbC1D1	Second Shell of distal Residue
*As*HbC1D5	13.2 ± 1.2	15.3 ± 2.1	0.86 ± 0.05	61 ± 0.7	0.23 ± 0.01	14.03 ± 0.7	46.97 ± 1	69.13 ± 1.6 5.65 ± 0.05		
G65I	17	32	0.52	13.5	0.49	6.6	6.9	34	*As*HbC1D5	Second Shell of distal Residue
I99V	18	8.8	2.1	16.1	0.74	8.8	7.3	18	*As*HbC1D5	Proximal side of heme
F138A	24	20	1.2	7.1	0.50	3.5	3.6	48	*As*HbC1D5	Proximal side of heme
Q8V	15	30	0.49	9.1	0.41	3.7	5.4	36	*As*HbC1D5	Distant from heme
W14F	16	24	0.66	9.5	0.43	3.9	5.15	36	*As*HbC1D5	Distant from heme

[a] The kinetic values of the SWMb and its mutants are measured based on O_2 as the ligand, whereas those of the recombinant protein are measured based on CO.

The rates of ligand exit from the interior of the protein or k_{escape} for *As*HbC1D1 and *As*HbC1D5 are 3.7- and 7.5-folds, respectively, higher than that of SWMb, which indicates that the ligand escapes faster from the inside of the domains than SWMb. To find the possible structural description for this behavior, we considered that ligands in myoglobin, are trapped in a "webbing" pocket of the distal site, and are surrounded by residues 28, 29, 32, 68, and 107 [35]. The size of this pocket determines the ligand entry equilibrium constant of the protein (K_{entry}), which is mathematically defined as k'_{entry} / k_{escape}. In Table 5, residues of these certain positions in *As*HbC1D1, *As*HbC1D5 and reference SWMb, as well as the corresponding values are summarized. As shown in the table, the smaller the residues, the lower the K_{entry}, hence, less ligand entry into the protein. If we compare the residues, we encounter that the residue in position 68 is the same in all proteins, and the size of residues in positions 28 and 29 in the recombinant proteins (Val and Phe) are almost equal with the size of corresponding residues in SWMb (Ile and Leu). Therefore, the difference in K_{entry} values is related to the size of the residue in positions 32 and 107. More specifically, in *As*HbC1D1 these positions are occupied by smaller residues (Val and Ser, respectively), where the ligand entry constant is the lowest (0.24 M^{-1}). In contrast, in SWMb due to the large size of residues in these two positions (Leu and Ile, respectively), the K_{entry} is the higher (5.39 M^{-1}). Moreover, in *As*HbC1D5, the size of the residues and the K_{entry} value (1.47 M^{-1}) are moderate. This is in accordance with Scott's proposal [35]. In addition to the size, the nature and orientation of the residues play an important role in the ligand entry and binding to the proteins. To further elucidate this, more structural and mutational analysis is necessary.

As given in Fig. 9 and Table 3, the direct electrochemical measurements reveal variation in the reduction potential ($E_{1/2}$) of the studied proteins. Interestingly, the reduction potential for *Af*Hb with 18 globin domains ($E_{1/2} = -0.13$ V versus SHE) is the highest, whereas the value of *As*HbC1D1 (−0.16 V), existing majorly in tetramer quaternary structure (Fig. 5), lies in between those of *Af*Hb and the single domain *As*HbC1D5 (−0.19 V). Thus, the higher number of globin domains stabilizes the iron in the heme in the Fe^{2+} state, i.e. 18 globin domains stabilize Fe^{2+} on about 1.5 kcal/mol ($\Delta G_{ET} = -nF\Delta E$) compared to the single domain. The latter can be important for minimization of methemoglobin (Fe^{3+}) formation, which is unable to bind molecular O_2.

5. Conclusion

To provide explicit answers to the above-mentioned questions, we cloned, expressed and purified two different recombinant globin domains in *E. coli* and purified the native Hb from the frozen animal. We utilized electron paramagnetic resonance, laser-flash photolysis and redox chemistry to investigate the physicochemical characteristics of two recombinant globin domains (*As*HbC1D1 and *As*HbC1D5) and the native one (*Af*Hb). Particularly, we focused on the comparison of the ligand binding kinetics, heme pocket structure and redox potential. UV–visible spectroscopy and analytical gel filtration of the recombinant proteins indicated single-heme globin-like proteins, which mediate ligand binding. However, there were difficulties in stability of *As*HbC1D5 in vitro. Moreover, the gel filtration indicated that there is equilibrium of tetramer and monomeric structure in *As*HbC1D1, while the *As*HbC1D5 just appears in monomeric structure.

Continuous Wave EPR showed that the heme pocket structure of the *Af*Hb is more closed than the reference myoglobin. Furthermore, the results of difference pulse voltammetry indicated a difference between the redox potential for recombinants and the native protein, emphasizing that the more the globin domains, the higher the redox potential.

In order to study the kinetics in more details, we calculated the association rate of CO binding together with geminate rebinding parameters in pseudo first order condition and the association and dissociation of O_2 in double replacement condition. The results showed that the *As*HbC1D1 has monophasic binding to CO, while the CO association to *As*HbC1D1 and *Af*Hb is biphasic. It is also indicated that *As*HbC1D1 has a slightly higher oxygen affinity than AsHbC1D5. It shows that they have a diverse role in ligand binding. When studying the full native molecule using ligand binding kinetics, we are faced with a large heterogeneity due to the presence of at least 18 globin domains. However the overall measurements would support an average oxygen affinity. Taken into account the fact that *Artemia* live in circumstances of variations in O_2 partial pressure due to difference in salinity, we would have expected a larger oxygen affinity. For example, it was reported that *Ascaris* Hb [41,42], due to its unique organization of the B10Tyr and E7Gln, has a lower O_2 dissociation rate and hence a higher affinity for O_2 to support life under low oxygen pressures. Hence, our results demonstrate that the *Af*Hb in contrast to *Ascaris* Hb supplies the O_2 requirement just by increasing the number of the ligand binding domains not by increasing the O_2 affinity. Indeed, the affinity is similar to SWMb.

Table 5
Ligand entry constant (K_{entry}) dependency on residue in *As*HbC1D1 and *As*HbC1D5 in comparison with SWMb based on [35].

	Positions					k'_{entry}	k_{escape}	K_{entry}
	28	29	32	68	107	$\mu M^{-1}\ s^{-1}$	μs^{-1}	M^{-1}
*As*HbC1D1	Val	Phe	Val	Val	Ser	5.82 ± 0.18	23.65 ± 4.2	0.24
*As*HbC1D5	Val	Phe	Leu	Val	Val	69.13 ± 1.6 5.56 ± 0.05	46.97 ± 1	1.47
SWMb[a]	Ile	Leu	Leu	Val	Ile	34 ± 7	6.3 ± 1	5.39

[a] The kinetic values are measured based on O_2 as ligand, whereas those of the recombinant protein are measured based on CO.

Transparency documents

The Transparency documents associated with this article can be found, in online version.

Acknowledgments

This work was supported by the Ministry of Science, Research and Technology of I. R. Iran and by the University of Antwerp. Q8

References

[1] G. Fermi, M.F. Perutz, B. Shaanan, R. Fourme, The crystal structure of human deoxyhaemoglobin at 1.74 A resolution, J. Mol. Biol. 175 (1984) 159–174.
[2] J.C. Kendrew, R.E. Dickerson, B.E. Strandberg, R.G. Hart, D.R. Davies, D.C. Phillips, V.C. Shore, Structure of myoglobin: a three-dimensional Fourier synthesis at 2 A. resolution, Nature 185 (1960) 422–427.
[3] D. Bashford, C. Chothia, A.M. Lesk, Determinants of a protein fold. Unique features of the globin amino acid sequences, J. Mol. Biol. 196 (1987) 199–216.
[4] M. Bolognesi, D. Bordo, M. Rizzi, C. Tarricone, P. Ascenzi, Nonvertebrate hemoglobins: structural bases for reactivity, Prog. Biophys. Mol. Biol. 68 (1997) 29–68.
[5] S.N. Vinogradov, D. Hoogewijs, X. Bailly, R. Arredondo-Peter, J. Gough, S. Dewilde, L. Moens, J.R. Vanfleteren, A phylogenomic profile of globins, BMC Evol. Biol. 6 (2006) 31.
[6] S.N. Vinogradov, D. Hoogewijs, X. Bailly, R. Arredondo-Peter, M. Guertin, J. Gough, S. Dewilde, L. Moens, J.R. Vanfleteren, Three globin lineages belonging to two structural classes in genomes from the three kingdoms of life, Proc. Natl. Acad. Sci. U. S. A. 102 (2005) 11385–11389.
[7] R.E. Weber, S.N. Vinogradov, Nonvertebrate hemoglobins: functions and molecular adaptations, Physiol. Rev. 81 (2001) 569–628.
[8] S.N. Vinogradov, L. Moens, Diversity of globin function: enzymatic, transport, storage, and sensing, J. Biol. Chem. 283 (2008) 8773–8777.
[9] K.E. Banister, A.C. Campbell, The Encyclopedia of Aquatic Life, Facts on File, Incorporated, Place Published, 1985.
[10] A.M. Manning, C.N.A. Trotman, W.P. Tate, Evolution of a polymeric globin in the brine shrimp *Artemia*, Nature 348 (1990) 653–656.
[11] C.N.A. Trotman, A.M. Manning, L. Moens, W.P. Tate, The polymeric hemoglobin molecule of *Artemia*: interpretation of translated cDNA sequence of nine domains, J. Biol. Chem. 266 (1991) 13789–13795.
[12] C.J. Vandenberg, C.M. Matthews, C.N. Trotman, Variant subunit specificity in the quaternary structure of *Artemia* hemoglobin, Mol. Biol. Evol. 19 (2002) 1288–1291.
[13] C.N. Trotman, A.M. Manning, J.A. Bray, A.M. Jellie, L. Moens, W.P. Tate, Interdomain linkage in the polymeric hemoglobin molecule of *Artemia*, J. Mol. Evol. 38 (1994) 628–636.
[14] C.M. Matthews, C.J. Vandenberg, C.N. Trotman, Variable substitution rates of the 18 domain sequences in *Artemia* hemoglobin, J. Mol. Evol. 46 (1998) 729–733.

[15] D.T. Chyou, V.L. Rawle, C.N. Trotman, Quaternary structure of *Artemia* haemoglobin II: analysis of T and C polymer alignment and interpolymer interface, BMC Struct. Biol. 7 (2007) 26–40.
[16] G. Wolf, M. Van Pachtenbeke, L. Moens, M.L. Van Hauwaert, Oxygen binding characteristics of *Artemia* hemoglobin domains, Comp. Biochem. Physiol. B: Comp. Biochem. 76 (1983) 731–736.
[17] J. D'Hondt, L. Moens, J. Heip, A. D'Hondt, M. Kondo, Oxygen-binding characteristics of three extracellular haemoglobins of *Artemia salina*, Biochem. J. 171 (1978) 705–710.
[18] J. Heip, L. Moens, M. Joniau, M. Kondo, Ontogenetical studies on extracellular hemoglobins of *Artemia salina*, Dev. Biol. 64 (1978) 73–81.
[19] J. Heip, L. Moens, M. Kondo, Effect of concentrations of salt and oxygen on the synthesis of extracellular hemoglobins during development of *Artemia salina*, Dev. Biol. 63 (1978) 247–251.
[20] V. Sugumar, N. Munuswamy, Physical, biochemical and functional characterization of haemoglobin from three strains of *Artemia*, Comp. Biochem. Physiol. A Mol. Integr. Physiol. 146 (2007) 291–298.
[21] D. Geelen, L. Moens, J. Heip, R. Hertsens, K. Donceel, J. Clauwaert, The structure of *Artemia* sp. haemoglobins—I. Isolation and characterization of oxygen binding domains obtained by limited tryptic digestion, Int. J. Biochem. 14 (1982) 991–1001.
[22] L. Moens, D. Geelen, M.L. Van Hauwaert, G. Wolf, R. Blust, R. Witters, R. Lontie, The structure of *Artemia* sp. haemoglobin. Cleavage of the native molecules into functional units by limited subtilisin digestion, Biochem. J. 223 (1984) 861–869.
[23] L. Moens, M. Kondo, Evidence for a dimeric form of *Artemia salina* extracellular hemoglobins with high-molecular-weight subunits, Eur. J. Biochem. 82 (1978) 65–72.
[24] D. Hoogewijs, E. Geuens, S. Dewilde, L. Moens, A. Vierstraete, S. Vinogradov, J. Vanfleteren, Genome-wide analysis of the globin gene family of *C. elegans*, IUBMB Life 56 (2004) 697–702.
[25] S. Dewilde, K. Mees, L. Kiger, C. Lechauve, M.C. Marden, A. Pesce, M. Bolognesi, L. Moens, Expression, purification, and crystallization of neuro- and cytoglobin, Methods Enzymol. 436 (2008) 341–357.
[26] S. Helbo, S. Dewilde, D.R. Williams, H. Berghmans, M. Berenbrink, A.R. Cossins, A. Fago, Functional differentiation of myoglobin isoforms in hypoxia-tolerant carp indicates tissue-specific protective roles, Am. J. Physiol. Regul. Integr. Comp. Physiol. 302 (2012) R693–R701.
[27] R.E. Weber, A. Fago, A.L. Val, A. Bang, M.L. Van Hauwaert, S. Dewilde, F. Zal, L. Moens, Isohemoglobin differentiation in the bimodal-breathing amazon catfish *Hoplosternum littorale*, J. Biol. Chem. 275 (2000) 17297–17305.
[28] J. Uzan, S. Dewilde, T. Burmester, T. Hankeln, L. Moens, D. Hamdane, M.C. Marden, L. Kiger, Neuroglobin and other hexacoordinated hemoglobins show a weak temperature dependence of oxygen binding, Biophys. J. 87 (2004) 1196–1204.
[29] S. Dewilde, A.I. Ioanitescu, L. Kiger, K. Gilany, M.C. Marden, S. Van Doorslaer, J. Vercruysse, A. Pesce, M. Nardini, M. Bolognesi, L. Moens, The hemoglobins of the trematodes *Fasciola hepatica* and *Paramphistomum epiclitum*: a molecular biological, physico-chemical, kinetic, and vaccination study, Protein Sci. Publ. Protein Soc. 17 (2008) 1653–1662.
[30] I. Birukou, R.L. Schweers, J.S. Olson, Distal histidine stabilizes bound O_2 and acts as a gate for ligand entry in both subunits of adult human hemoglobin, J. Biol. Chem. 285 (2010) 8840–8854.
[31] J.S. Olson, E.W. Foley, D.H. Maillett, E.V. Paster, Measurement of rate constants for reactions of O_2, CO, and NO with hemoglobin, Methods Mol. Med. 82 (2003) 65–91.
[32] J. Haladjian, P. Bianco, F. Nunzi, M. Bruschi, A permselective-membrane electrode for the electrochemical study of redox proteins. Application to cytochrome c552 from *Thiobacillus ferrooxidans*, Anal. Chim. Acta 289 (1994) 15–20.
[33] É. Lojou, P. Bianco, Membrane electrodes can modulate the electrochemical response of redox proteins — direct electrochemistry of cytochrome c, J. Electroanal. Chem. 485 (2000) 71–80.
[34] C.P. Scholes, K.M. Falkowski, S. Chen, J. Bank, Electron nuclear double resonance (ENDOR) of bis(imidazole) ligated low-spin ferric heme systems, J. Am. Chem. Soc. 108 (1986) 1660–1671.
[35] E.E. Scott, Q.H. Gibson, J.S. Olson, Mapping the pathways for O_2 entry into and exit from myoglobin, J. Biol. Chem. 276 (2001) 5177–5188.
[36] R.E. Cashon, M.E. Vayda, B.D. Sidell, Kinetic characterization of myoglobins from vertebrates with vastly different body temperatures, Comp. Biochem. Physiol. B Biochem. Mol. Biol. 117 (1997) 613–620.
[37] E. Antonini, M. Brunori, Hemoglobin and Myoglobin in Their Reactions With Ligands, North-Holland Pub. Co, 1971. (Place Published).
[38] A. Pesce, M. Nardini, S. Dewilde, L. Capece, M.A. Marti, S. Congia, M.D. Salter, G.C. Blouin, D.A. Estrin, P. Ascenzi, L. Moens, M. Bolognesi, J.S. Olson, Ligand migration in the apolar tunnel of *Cerebratulus lacteus* mini-hemoglobin, J. Biol. Chem. 286 (2011) 5347–5358.
[39] G. Amiconi, E. Antonini, M. Brunori, H. Formaneck, R. Huber, Functional properties of native and reconstituted hemoglobins from *Chironomus thummi thummi*, Eur. J. Biochem. FEBS 31 (1972) 52–58.
[40] M.D. Salter, K. Nienhaus, G.U. Nienhaus, S. Dewilde, L. Moens, A. Pesce, M. Nardini, M. Bolognesi, J.S. Olson, The apolar channel in *Cerebratulus lacteus* hemoglobin is the route for O_2 entry and exit, J. Biol. Chem. 283 (2008) 35689–35702.
[41] A. Pesce, S. Dewilde, L. Kiger, M. Milani, P. Ascenzi, M.C. Marden, M.L. Van Hauwaert, J. Vanfleteren, L. Moens, M. Bolognesi, Very high resolution structure of a trematode hemoglobin displaying a TyrB10–TyrE7 heme distal residue pair and high oxygen affinity, J. Mol. Biol. 309 (2001) 1153–1164.
[42] E.S. Peterson, S. Huang, J. Wang, L.M. Miller, G. Vidugiris, A.P. Kloek, D.E. Goldberg, M.R. Chance, J.B. Wittenberg, J.M. Friedman, A comparison of functional and structural consequences of the tyrosine B10 and glutamine E7 motifs in two invertebrate hemoglobins (*Ascaris suum* and *Lucina pectinata*), Biochemistry 36 (1997) 13110–13121.

Please cite this article as: H.A. Borhani, et al., Kinetic properties and heme pocket structure of two domains of the polymeric hemoglobin of *Artemia* in comparison with the native molecule..., Biochim. Biophys. Acta (2015), http://dx.doi.org/10.1016/j.bbapap.2015.05.007